IEEJ Journal of Industry Applications
Vol.10 No.4 pp.428–435 DOI: 10.1541/ieejjia.20004635

Paper

Quasi Multirate Feedforward Current Control toward Nyquist Frequency of PWM for SPMSM

Shona Noguchi* Student Member, Masahiro Mae* Student Member
Hiroshi Fujimoto*a) Senior Member

(Manuscript received May 12, 2020, revised Feb. 24, 2021)
J-STAGE Advance published date : April 23, 2021

A high-bandwidth current controller is necessary to suppress torque ripple. To drive motors at high speeds, the reference-value-tracking performance must be guaranteed. To ensure the reference-value-tracking performance around the Nyquist frequency, the proposed method samples reference values twice more than the conventional multirate feedforward control for a second-order system. We have previously proposed a current controller based on the perfect tracking control. However, there is still room to improve the reference value tracking performance; therefore, a new approach based on the quasi multirate feedforward current control has been proposed and applied to permanent magnet synchronous motors. The proposed method doubles the tracking points of the reference current waveform compared with the conventional methods. The enhancement of the proposed approach has been demonstrateted using simulations and experimental verifications.

Keywords: permanent magnet synchronous motor (PMSM), current control, perfect tracking control, quasi multirate feedforward control, tracking performance

1. Introduction

The development of electrified vehicles such as hybrid vehicles (HVs) and electric vehicles (EVs) for the prevention of air pollution and global warming is increasing. Furthermore, some countries have declared the prohibition of selling gasoline and diesel engine cars [1]. It is therefore expected that the number of electrified vehicles will increase in the future [2].

In the use of electric motors, the motor noise and vibration are well-known problems. Such problems are tackled by the car manufacturer, and it has been reported that they are suppressed by reducing the excitation force with an optimized magnetic circuit [3]. Torque ripple, one of the causes of such problems, is generated from the spatial harmonics included in the permanent magnet flux distribution, such as the distorted back electromotive force (EMF) [4].

There are two approaches used to suppress the torque ripple. One is a mechanical approach, of which skew is the best-known method [5]. Although this is a simple way to suppress the torque ripple, there are disadvantages in the processing cost and the reduction of the torque output. By contrast, the control approach has no such disadvantages because additional processing is unnecessary. Therefore, we have taken a control approach.

Several papers have reported the suppression of the torque ripple. For example, it was reported that the torque ripple is suppressed with a Kalman filter to assume the actual electric angle to transform between the dq-axis and 3-phase model [6]. The torque ripple reduction effect is applied through the experiment with motors for actual EVs at a speed of up to 300 rpm. Another study reported that the torque ripple is suppressed by injecting the compensation current determined by the gradient descent optimization (GDO) [7]. The compensation signal determined by the GDO can suppress the torque ripple at minimal current. Another study is reported that the feedforward controller based on the perfect tracking control (PTC) can improve the reference value tracking performance [8] and suppress the torque ripple at a higher speed [9][10]. However, they have not discussed the torque ripple reduction effect at a high-speed range of more than 1000 rpm and the tracking performance of the current control.

Though an experiment on motors used for actual EVs, it was reported that the low current control bandwidth is a problem causing the noise and vibration [11]. Thus, it is necessary for an application to reduce the noise and vibration within a wide bandwidth through a control approach to broaden the bandwidth of the current control. In general, the proportional-integral (PI) feedback control is used as the current control of a motor. However, as a problem of the PI control when the reference current is steeply changed, the output current cannot follow it owing to the limitation of the high bandwidth control from the modeling errors. Therefore, the proposed method is designed with a feedforward controller for guaranteeing the tracking performance of the reference value to the drive motors.

The proposed feedforward controller is designed using the PTC. Furthermore, a quasi multirate deadbeat control is proposed as a new digital control method [12]. This method applies a new feedforward control approach using multirate feedforward control, which is improved by increasing the

a) Correspondence to: Hiroshi Fujimoto. E-mail: fujimoto@k.u-tokyo.ac.jp
* The University of Tokyo
5-1-5, Kashiwanoha, Kashiwa, Chiba 227-8561, Japan

sampling period of the double reference value [13]. Although the effectiveness of the proposed current control method has been verified through a simulation and experiment, in this paper the effectiveness while the motor is rotated is discussed based on the frequency response of the tracking error when compared to the PI and the multirate feedforward control. In this study, the authors improved the tracking performance of the reference value by adopting the quasi multirate control. This paper is organized as follows: First, the control theory is described in Section 2. The conditions of the simulation and its result are discussed in Section 3. The experimental results are provided in Section 4. Finally, some concluding remarks are presented in Section 5.

2. Control System Design

2.1 PWM Hold Model Fig. 1 shows the circuit diagram of the single-phase inverter. It outputs either 0 V or $\pm E$ V as shown in Fig. 2. Fig. 3 shows the hold models. A zero-order hold (ZOH) is commonly used for the discretization of a system. The ZOH outputs $V[k]$ at a sampling point k as the discretized value. However, a more exact plant model compared to the ZOH can be obtained by treating the pulse width as the control input and discretizing it. To achieve this, a pulse width modulation (PWM) hold is introduced [14]. The control system is discretized with the on-time $\Delta T[k]$ as a control input $u[k]$.

The state-space model with the controllable canonical form

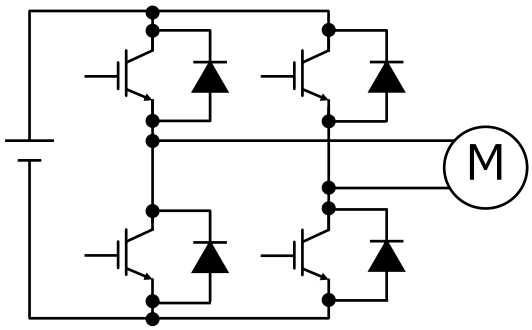

Fig. 1. Circuit diagram of single-phase inverter

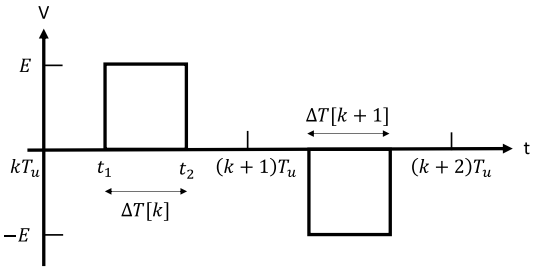

Fig. 2. Output of single-phase inverter

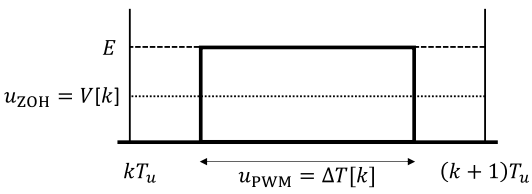

Fig. 3. DC voltage waveform discretized using PWM hold

(1) and (2) can be described using the PWM hold,

$$\boldsymbol{x[k+1]} = \boldsymbol{A_s x[k]} + \boldsymbol{b_s}\Delta T[k], \cdots\cdots\cdots\cdots (1)$$

$$y[k] = \boldsymbol{c_s x[k]}, \cdots\cdots\cdots\cdots\cdots\cdots\cdots\cdots (2)$$

where $\boldsymbol{A_s} = e^{\boldsymbol{A_c} T_u}$, $\boldsymbol{b_s} = e^{\boldsymbol{A_c} T_u/2}\boldsymbol{b}E$, $\boldsymbol{c_s} = \boldsymbol{c_c}$, and if $\Delta T < 0$, then the output voltage will be $-E$.

2.2 Multirate Feedforward Control The multirate feedforward control based on the perfect tracking control (PTC) is described to design the proposed method. The PTC is the control system that tracks reference values without errors at every sampling point [15]. Fig. 5 shows the block diagram of PTC. It was reported that this phenomenon is achieved by the multirate feedforward controller based on the PTC [16]. This control system is the two degrees of the freedom composed by the feedforward and the feedback controller.

If there are disturbances or modeling errors, the feedback controller C_{PI} suppresses them. There are two samplers for the reference r and the output y, and one holder for the input u, in a digital control system. Therefore, the sampling parameters are notated as T_r, T_y, and T_u, which represent the sampling periods of r, y, and u, respectively.

Fig. 4 shows the sampling period in a multirate system. Here, l is defined as the index of the reference sampling point of a reference value. The state equation is described up to n samples ahead by lifting. Here, n is the plant order. The controllable canonical forms (1) and (2) are discretized with the sampling period T_u. The discretized $\boldsymbol{A}$, $\boldsymbol{B}$, $\boldsymbol{C}$, and $\boldsymbol{D}$ matrices of the control system are

$$\left(\begin{array}{c|c} \boldsymbol{A} & \boldsymbol{B} \\ \hline \boldsymbol{C} & \boldsymbol{D} \end{array}\right) = \left(\begin{array}{c|ccc|c} \boldsymbol{A_s}^n & \boldsymbol{A_s}^{n-1}\boldsymbol{b_s} & \cdots & \boldsymbol{A_s b_s} & \boldsymbol{b_s} \\ \hline \boldsymbol{c_s} & 0 & \cdots & 0 & 0 \\ \boldsymbol{c_s A_s} & \boldsymbol{c_s b_s} & \cdots & 0 & 0 \\ \vdots & \vdots & \ddots & \vdots & \vdots \\ \boldsymbol{c_s A_s}^{n-1} & \boldsymbol{c_s A_s}^{n-2}\boldsymbol{b_s} & \cdots & \boldsymbol{c_s b_s} & 0 \end{array}\right). \cdots\cdots\cdots\cdots (3)$$

The controllability matrix is a full rank because the system is controllable, and thus $\boldsymbol{B}$ matrix is a non-singular matrix. The control input $\boldsymbol{u_o}[l]$ is described as follows from (3) to achieve PTC.

$$\begin{aligned}\boldsymbol{u_o}[l] &= \boldsymbol{B^{-1}}(\boldsymbol{I} - z^{-1}\boldsymbol{A})\boldsymbol{x[l+1]} \\ &= \left(\begin{array}{c|c} \boldsymbol{0} & \boldsymbol{I} \\ \hline \boldsymbol{-B^{-1}A} & \boldsymbol{B^{-1}} \end{array}\right)\boldsymbol{x[l+1]}, \cdots\cdots\cdots\cdots (4)\end{aligned}$$

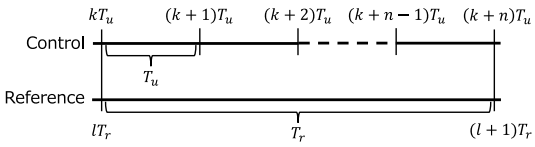

Fig. 4. Multirate sampling periods

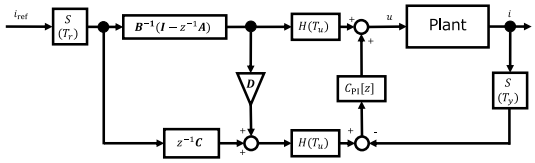

Fig. 5. Block diagram of PTC

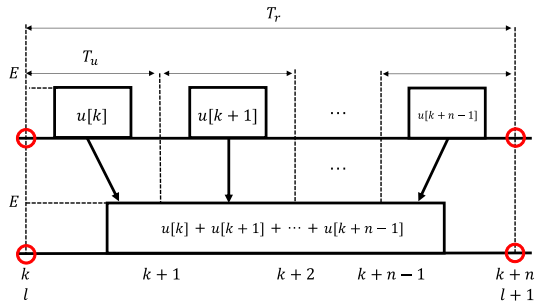

Fig. 6. Principle of quasi multirate control

$$y_o[l] = z^{-1}\boldsymbol{Cx[l+1]} + \boldsymbol{Du}_o[l], \quad \cdots\cdots\cdots\cdots\cdots (5)$$

where $z = e^{sT_r}$. The feedforward control input is generated by (4) with one-sample ahead desired state trajectory $\boldsymbol{x[l+1]}$. This guarantees the perfect tracking of the nominal plant at every period T_r.

2.3 Quasi Multirate Feedforward Control The proposed quasi multirate feedforward control is described in this subsection. Fig. 6 shows the principle of the quasi multirate control. The on-time is generated between the sampling points of index l corresponding to the control period. In the multirate control system, $\boldsymbol{u_o}[l]$ of (4) consists of

$$\begin{aligned}\boldsymbol{u_o}[l] &= [u_1\ u_2\ \ldots\ u_n]^{\mathsf{T}} \\ &= [u[k]\ u[k+1]\ \ldots\ u[k+n-1]]^{\mathsf{T}}, \cdots\cdots\cdots (6)\end{aligned}$$

where each control input u is

$$\begin{aligned}u[k] &= \left(B_{11}^{-1} - z^{-1}\sum_{m=1}^{n} B_{1m}^{-1}A_{m1}\right)x_1[l+1], \\ u[k+1] &= \left(B_{22}^{-1} - z^{-1}\sum_{m=1}^{n} B_{2m}^{-1}A_{m2}\right)x_2[l+1], \\ &\vdots \\ u[k+n-1] &= \left(B_{nn}^{-1} - z^{-1}\sum_{m=1}^{n} B_{nm}^{-1}A_{mn}\right)x_n[l+1]. \\ &\qquad\qquad\qquad\qquad\qquad\qquad \cdots\cdots\cdots\cdots (7)\end{aligned}$$

Here, A_{mn} is the element of the matrix $\boldsymbol{A}$ at the mth row and nth column and B_{nm}^{-1} is the element of the inverse matrix of $\boldsymbol{B}$ at the nth row and mth column. From (7), the equation at a sampling point of the reference value lT_r is described as follows:

$$u_o'[l] = u[k] + u[k+1] + \cdots + u[k+n-1]. \cdots\cdots (8)$$

Thus, PWM pulses are combined into one pulse, and $u_o'[l]$ described by combining PWM pulses is a new control input [17].

A single pulse can be obtained as shown in Fig. 6. As a result, the number of output pulses of the quasi multirate feedforward control is smaller than that of the multirate feedforward control under the condition in which the reference sampling period is the same. This is because the average output voltage between kT_u and $(k+n)T_u$ is the same as before combining the pulses. However, the response between sample points of a reference trajectory can deteriorate because none of the added output pulses are generated accurately when considering the state at that time.

To sample the reference value n times as fast as the normal multirate control beforehand, the number of switches can be increased. Therefore, the tracking performance of a reference value can be improved by designing the multirate controller based on the PTC and oversampling reference values without changing a carrier frequency.

3. Simulation

3.1 Plant Modeling In this study, SPMSM is the target plant, and its dq coordinate model is shown in Fig. 7. Now, if the d-axis current $i_d = 0$ is maintained by the current controller and the decoupling control, the plant model on the q-axis can be assumed to be a DC motor, as shown in Fig. 8. The transfer function of the controlled system can be expressed in the same way as the DC motor. The transfer function is from the voltage input to the current output in the continuous-time. Because the transfer function from the voltage input to the current output must include the feedback loop owing to the effect of the back EMF, the plant model would be the second-order plant model, which is given as follows:

$$\frac{i}{v} = \frac{Js + B}{JLs^2 + (JR + LB)s + (BR + K_eK_t)}. \cdots\cdots\cdots (9)$$

The controllable canonical form of this model is described as follows with the state variable $\boldsymbol{x}(t) = [x\ \dot{x}]^{\mathsf{T}}$.

$$\dot{\boldsymbol{x}}(t) = \boldsymbol{A_c x}(t) + \boldsymbol{b_c}u(t), \cdots\cdots\cdots\cdots (10)$$

$$y(t) = \boldsymbol{c_c x}(t), \cdots\cdots\cdots\cdots (11)$$

where

$$\boldsymbol{A_c} = \begin{bmatrix} 0 & 1 \\ -\frac{BR+K_eK_t}{JL} & -\frac{JR+LB}{JL} \end{bmatrix}, \cdots\cdots\cdots (12)$$

$$\boldsymbol{b_c} = \begin{bmatrix} 0 & \frac{1}{JL} \end{bmatrix}^{\mathsf{T}}, \cdots\cdots\cdots (13)$$

$$\boldsymbol{c_c} = [B\ J]. \cdots\cdots\cdots (14)$$

As described in the equations above, the simulation is conducted by applying multirate feedforward control as a conventional method and the quasi multirate feedforward control as a proposed method to the SPMSM plant model, which is defined through (9).

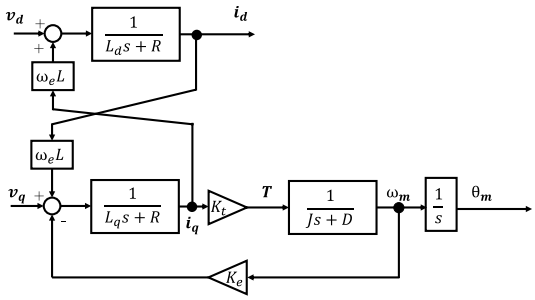

Fig. 7. Block diagram of SPMSM at dq-axis

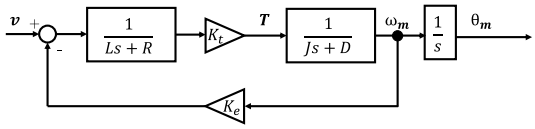

Fig. 8. Block diagram of DC motor

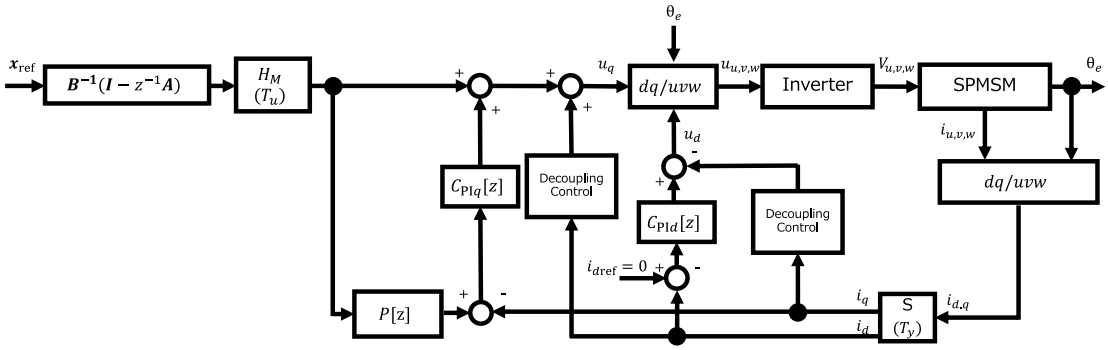

Fig. 9. Current control based on PTC

Table 1. Motor parameters

Parameter	Value
Resistance $R[\Omega]$	0.1567
Inductance L [mH]	3.65
Inertia J [kg · m^2]	9.084×10^{-4}
Viscous resistance D [N · m · s/rad]	4.00×10^{-4}
Pole pairs P	4
Induced electromotive voltage K_e [V · s/rad]	0.1727
Torque constant K_t [N · m/A]	0.1727
Carrier frequency f_c [kHz]	10
DC input voltage of inverter E [V]	250
Reference current input I_{qref} [A]	1

3.2 Feedforward Controller Design Fig. 9 shows the block diagram used in the simulation. The simulation model is designed as a 3-phase model. Table 1 shows the parameters of the simulation. The plant model is a second-order model owing to a feedback loop by the back EMF, and therefore the transfer function from the voltage input to the current output is described as (9).

The $\boldsymbol{A}, \boldsymbol{B}$ matrices of the multirate feedforward controllers and $P[z]$ are designed by the dq-axis model of the SPMSM. They are discretized using the PWM hold. The controllable canonical form is described through the transfer function of the plant (9) and is then substituted for (1) and (2) to determine the parameters under the discrete-time. The parameters are substituted for the equation (3)–(5) to determine the $\boldsymbol{A}, \boldsymbol{B}$ matrices of the multirate feedforward controllers.

Fig. 10 shows a pulse pattern comparison between a multirate and the quasi multirate feedforward control. Fig. 10 assumes that the plant order is 2, for example. The sampling period of the reference value through the proposed method T_r' can be reduced compared to a conventional multirate feedforward control. In Fig. 10, T_r' is defined as $T_r/2$, and the feedforward calculation is held every $T_r'/2$, whereas the pulses are generated at T_r', which equals to the carrier frequency. Thus, the calculation of the control input of the proposed method considered with an oversampling is increased twofold compared with a conventional multirate feedforward control.

3.3 Feedback Controller Design The current controller C_{PI} is designed as a PI feedback controller. The gains of the PI feedback controller are described as follows.

$$K_p = 2\zeta\omega L - R, \quad \cdots\cdots (15)$$

$$K_i = \omega^2 L. \quad \cdots\cdots (16)$$

Here, the poles of the PI feedback controller are placed as a closed system, which becomes a Butterworth filter [18],

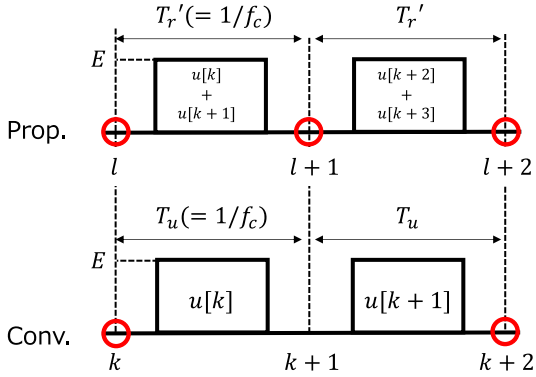

Fig. 10. Comparison of PWM pulse pattern between quasi multirate and multirate control

$$\omega = 2\pi f, \quad \cdots\cdots (17)$$

$$\zeta = \frac{1}{\sqrt{2}}. \quad \cdots\cdots (18)$$

The cut-off frequency of the closed-loop system f is designed at 400 Hz. Thus, the transfer function of this feedback controller is as follows:

$$C_{\mathrm{PI}} = K_p + K_i \frac{1}{s}. \quad \cdots\cdots (19)$$

For the experiment, the transfer function is discretized by the Tustin transform when considering the ZOH.

3.4 Simulation Results The frequencies of the reference current f_{ref} are 10, 100, 1000, and 2500 Hz in the simulation. The sampling periods of the multirate feedforward control are $T_r = 200\,\mu$s and $T_u = 100\,\mu$s, respectively. By contrast, T_r' of the quasi multirate feedforward control is 100 µs without changing the carrier frequency f_c. This simulation assumes that the load motor is rotating at a speed in which the frequency of the 6th harmonics is as same as that of the input current. The input rotation speed is calculated by the following:

$$\omega = \frac{60 f_{\mathrm{ref}}}{6P}. \quad \cdots\cdots (20)$$

The simulation results are given in Fig. 11, which shows the current waveform of the PI control, the multirate feedforward control, and the quasi multirate feedforward control. The conventional methods apply PI control and multirate feedforward control, and the proposed method applies the quasi multirate feedforward control described in this paper. Although the waveform changes depending on phases,

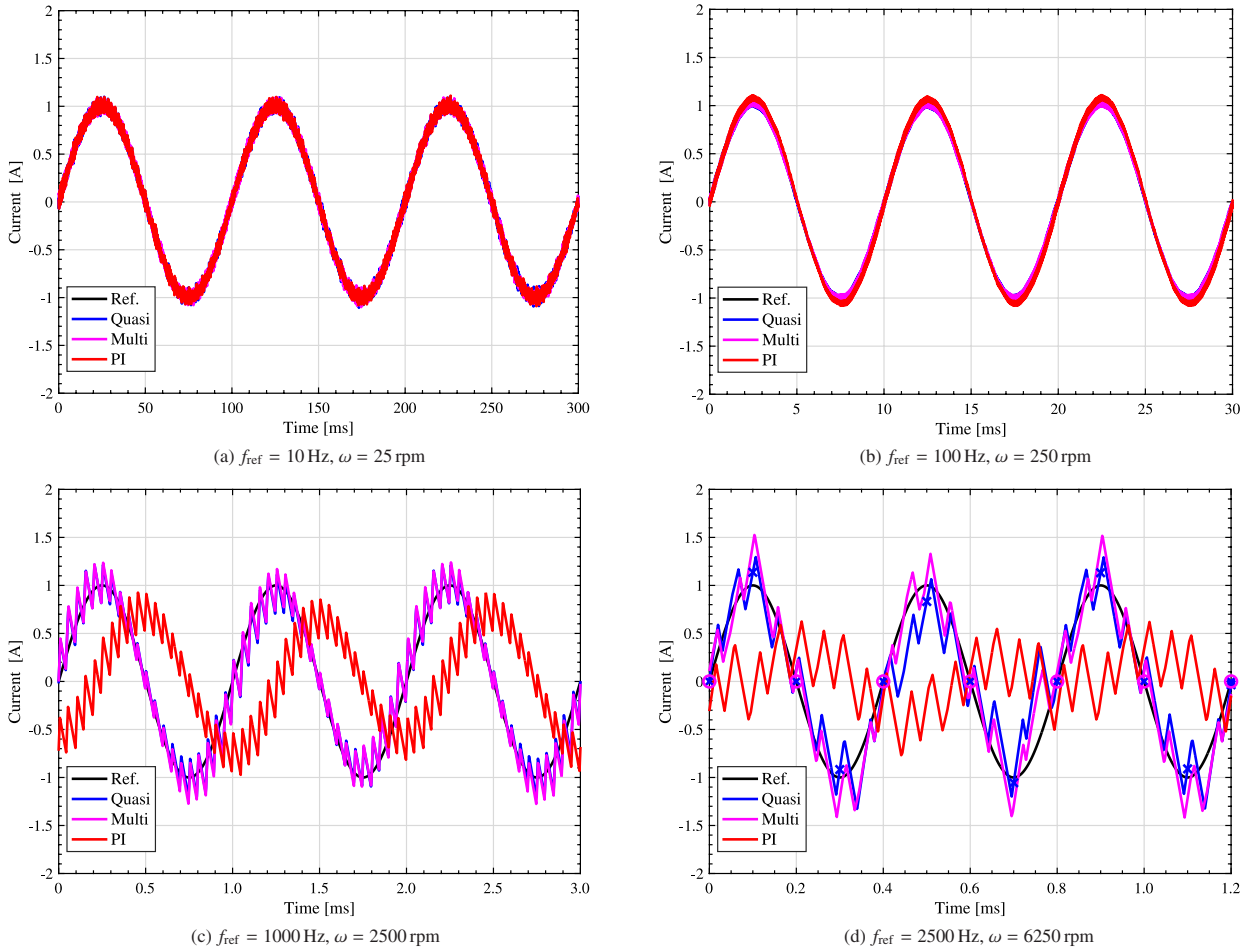

(a) $f_{\mathrm{ref}} = 10\,\mathrm{Hz}$, $\omega = 25\,\mathrm{rpm}$

(b) $f_{\mathrm{ref}} = 100\,\mathrm{Hz}$, $\omega = 250\,\mathrm{rpm}$

(c) $f_{\mathrm{ref}} = 1000\,\mathrm{Hz}$, $\omega = 2500\,\mathrm{rpm}$

(d) $f_{\mathrm{ref}} = 2500\,\mathrm{Hz}$, $\omega = 6250\,\mathrm{rpm}$

Fig. 11. Simulation q-axis waveform of 6th current control

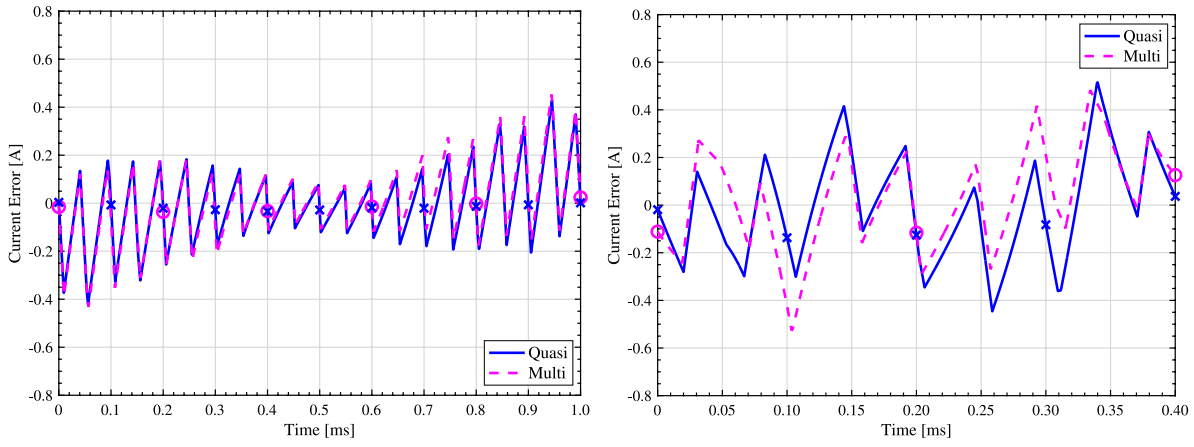

(a) $f_{\mathrm{ref}} = 1000\,\mathrm{Hz}$, $\omega = 2500\,\mathrm{rpm}$

(b) $f_{\mathrm{ref}} = 2500\,\mathrm{Hz}$, $\omega = 6250\,\mathrm{rpm}$

Fig. 12. Simulation q-axis current error between input and output

the simulation results are as shown in Fig. 11 when the phase difference is 0. The PI control cannot track the reference value as it changes more steeply from Fig. 11. However, the multirate feedforward control and the quasi multirate feedforward control can track the reference value under 1000 Hz. Therefore, they can track the reference value under high-bandwidth. Moreover, Fig. 11(d) shows a comparison between the multirate feedforward control as the conventional method and the quasi multirate feedforward control as the proposed method at the Nyquist frequency of the multirate control. The circle mark indicates the sampling point of the multirate feedforward control, and the cross mark is the sampling point of the quasi multirate feedforward control. The proposed method can track the reference trajectory because its waveform is closer to the reference waveform.

Moreover, the error between the input and output current of the multirate feedforward control and the quasi multirate feedforward control is shown in Fig. 12. From Fig. 12, the quasi multirate feedforward control can cross nearly 0 at every carrier period compared to the multirate feedforward control. Theoretically, the tracking error can be 0 at every sampling point T_r using the conventional method and T_r' by the

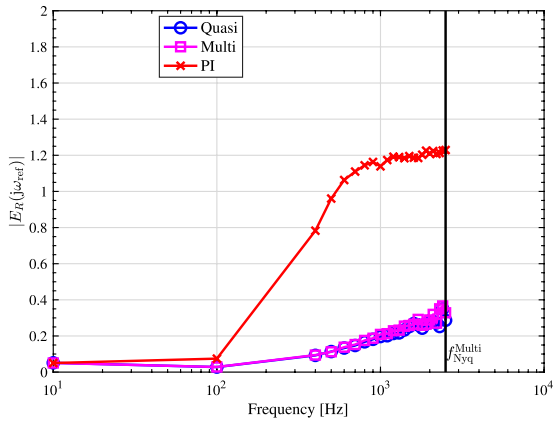

Fig. 13. Simulation frequency response of inter-sample tracking error

$$|E_R(j\omega_{ref})| = \frac{\sqrt{\frac{1}{T}\int_0^T e^2(t)dt}}{\sqrt{\frac{1}{T}\int_0^T (i_{qref}(t))^2 dt}} \cdots\cdots\cdots\cdots\cdots\cdots (21)$$

Here, $T = 1/f_{ref}$ and $e(t) = i_{qref}(t) - i_q^{output}(t)$, where $i_q^{output}(t)$ is the output currents controlled by the PI control, the multirate feedforward control, and the quasi multirate feedforward control. From Fig. 13, the RMS value ratio (21) between the reference and the error of the quasi multirate feedforward control is smaller than the multirate feedforward control as the frequency of the reference value steeply changes. Thus, the proposed method can track the reference value more accurately. However, each max error value in Fig. 12 is larger than the multirate feedforward control. It is considered that the quasi multirate feedforward control contains the modeling error because the control inputs of the quasi multirate proposed method, respectively. However, this phenomenon was not observed in this simulation because the motor is rotating at high-speed, and thus the coordinate transformation error can appear because the electric angle θ_e steeply changes [19].

Furthermore, Fig. 13 shows the ratio of the reference and the error value by the root mean square (RMS). The ratio of the RMS is calculated as

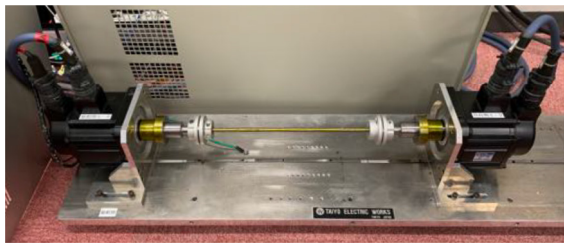

Fig. 14. Experimental setup (SPMSM)

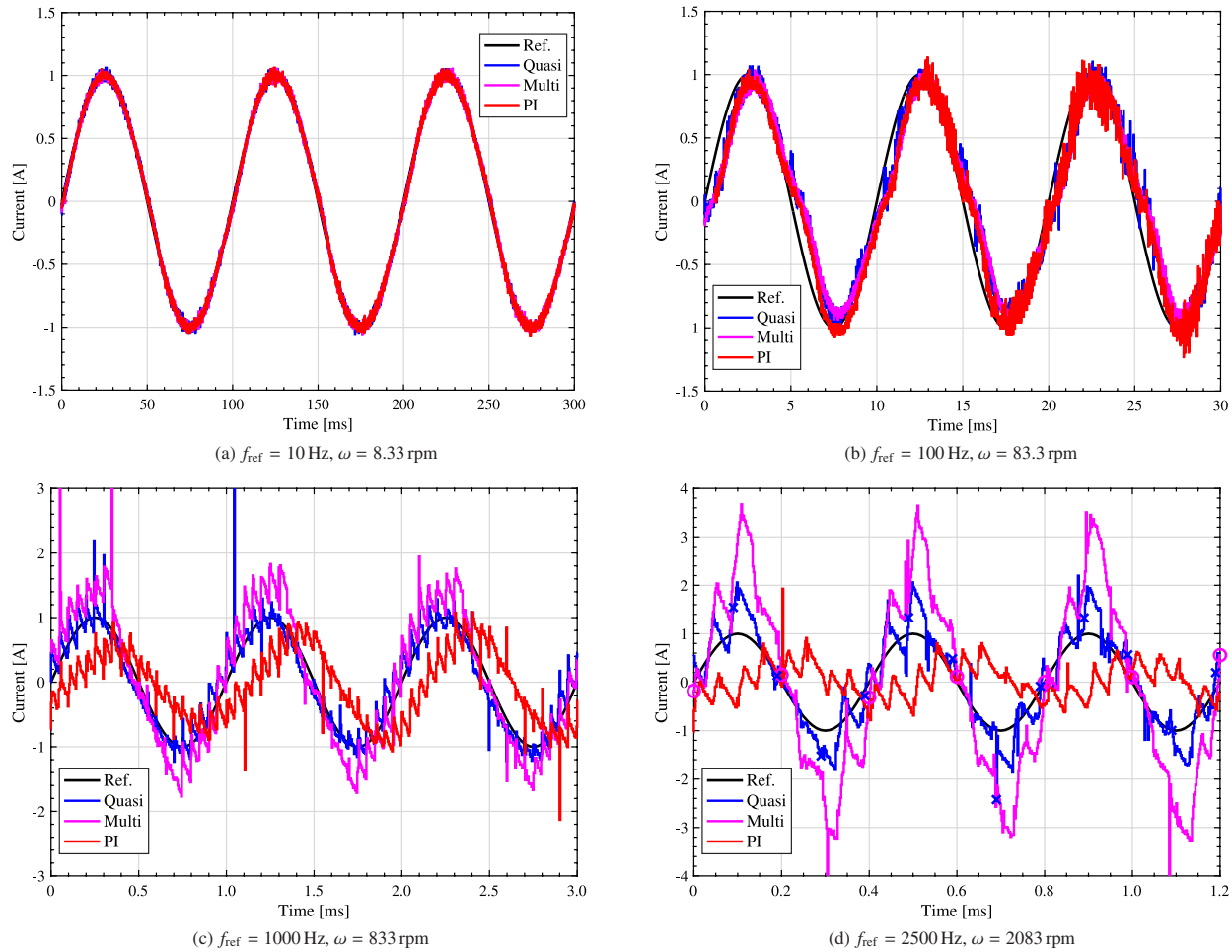

(a) f_{ref} = 10 Hz, ω = 8.33 rpm

(b) f_{ref} = 100 Hz, ω = 83.3 rpm

(c) f_{ref} = 1000 Hz, ω = 833 rpm

(d) f_{ref} = 2500 Hz, ω = 2083 rpm

Fig. 15. Experimental q-axis waveform of 18th current control

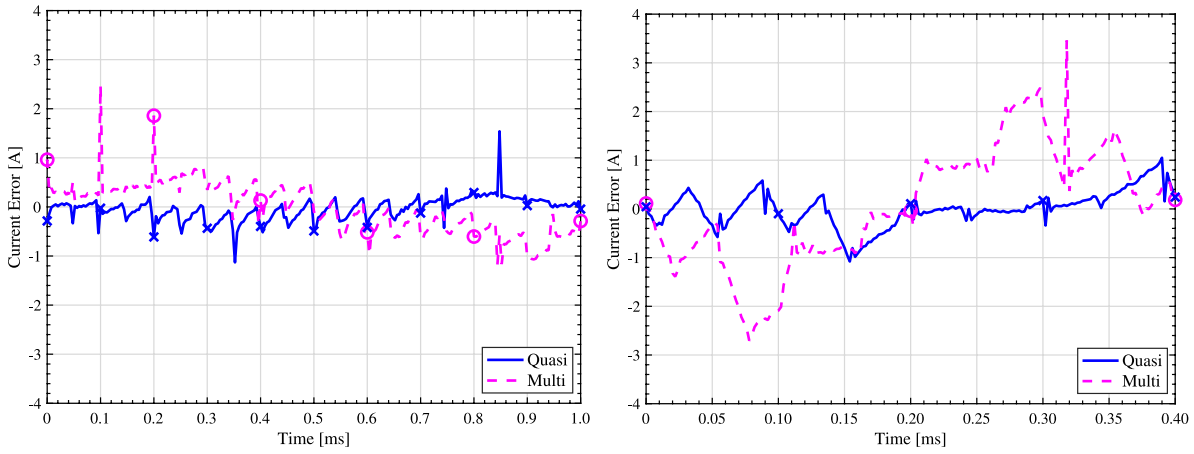

(a) $f_{\mathrm{ref}} = 1000\,\mathrm{Hz}$, $\omega = 833\,\mathrm{rpm}$ (b) $f_{\mathrm{ref}} = 2500\,\mathrm{Hz}$, $\omega = 2083\,\mathrm{rpm}$

Fig. 16. Experimental q-axis current error between input and output

feedforward control are the sum of two pulses.

From these simulation results, the proposed method that samples twice more than the conventional method can track the reference trajectory more accurately without changing the carrier frequency. These results verify the effectiveness of the proposed method.

4. Experiment

Fig. 14 shows the motor bench used in the current control of the experimental validation. Although the parameters are the same as the simulation, the rotation speed of the test motor has been set at a speed of 1/3 of the rotation speed obtained by (20) assuming the 18th harmonic in this experiment. The current waves are obtained as follows: First, they are observed using an oscilloscope. Next, the electric angle θ_e is obtained on the sampling points. Finally, the coordinate transformation is processed with the observed current waves and θ_e, which is interpolated linearly. The PI control and the multirate feedforward control are demonstrated as the conventional methods, and the quasi multirate feedforward control is the proposed method.

The experimental results of the current waveform are shown in Fig. 15. From Fig. 15, the current controllers based on the multirate feedforward control improved the tracking performance better than the PI control, similar to the simulation results. Moreover, the proposed method successfully demonstrated a better reference tracking performance than the conventional methods at a high-bandwidth, as indicated in Fig. 15(d).

Furthermore, the tracking error between the input and output current of the multirate feedforward control and the quasi multirate feedforward control is shown in Fig. 16. The proposed method can track a reference trajectory more accurately for less tracking error compared to the conventional method, similar to the simulation shown in Fig. 16. Furthermore, Fig. 17 shows the frequency response of the RMS ratio between the reference and the error values from the results in Fig. 15. The RMS ratio is calculated by (21) as $T = 3/f_{\mathrm{ref}}$. The RMS ratio of the proposed method is less than that of the conventional methods, and therefore the proposed method can improve the reference tracking performance at a high-bandwidth without changing the carrier frequency. Thus, the

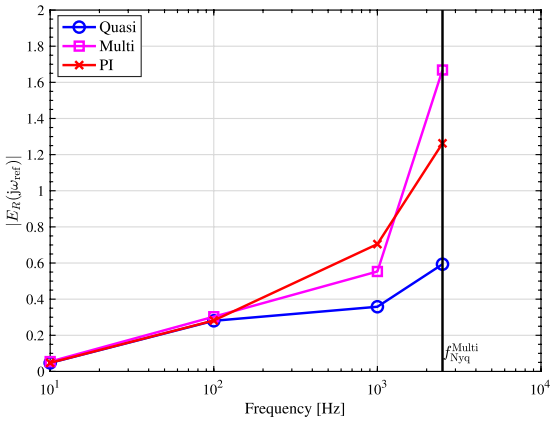

Fig. 17. Experimental frequency response of inter-sample tracking error

effectiveness of the proposed method is also validated, similar to the simulation results.

5. Conclusion

A new current control method based on the quasi multirate feedforward control is proposed in this paper. Although previous research shows that the multirate feedforward controller can improve the output tracking performance compared with the PI control, the proposed method has an improved tracking performance with an increase in the sampling period of reference trajectory double that of the conventional methods. The effectiveness of the proposed method has been demonstrated in simulations and experiments.

The torque ripple suppression effect by the PTC based on a reference value oversampling similar to quasi multirate feedforward control is confirmed in [19]. However, the experiment was conducted using a motor bench, and thus a future study will be conducted to demonstrate the effectiveness of the proposed method for electric vehicle motors.

References

(1) MLIT and METI: “The current status and issues of fuel efficiency regulations for vehicles”, https://www.mlit.go.jp/common/001224511.pdf, Accessed in January 16th (2020)

(2) Bloomberg NEF: “Electric vehicles to be 35% of global new car sales by 2040”, https://about.bnef.com/blog/electric-vehicles-to-be-35-of-global-new-car-sales-by-2040/, Accessed in February 13th (2021)
(3) T. Tanno, S. Ishikawa, M. Abe, S. Oki, and T. Nakada: “Developfment of an Interior Permanent Magnet Synchronous Motor for a Newly Developed Electric Vehicle”, EVTeC and APE Japan (2014)
(4) N. Nakao, K. Tobari, T. Sugino, Y. Ito, M. Mishima, and D. Maeda: “Minimizating Pulsating Torque in PMSM Drives by using Feedforward-based Compensation and Flux-harmonic Estimation”, IEEE Energy Conversion Congress and Exposition, pp.3030–3037 (2020)
(5) R. Islam, I. Husain, A. Fardoun, and K. McLaughlin: “Permanent-Magnet Synchronous Motor Magnet Designs With Skewing for Torque Ripple and Cogging Torque Reduction”, IEEE Transactions on Industry Applications, Vol.45, No.1, pp.152–160 (2009)
(6) Y. Mao, S. Zuo, and J. Cao: “Effects of Rotor Position Error on Longitudinal Vibration of Electric Wheel System in In-Wheel PMSM Driven Vehicle”, IEEE/ASME Transactions on Mechatronics, Vol.23, No.3, pp.1314–1325 (2018)
(7) L. Yan, Y. Liao, H. Lin, and J. Sun: “Torque ripple suppression of permanent magnet synchronous machines by minimal harmonic current injection”, IET Power Electronics, Vol.12, No.6, pp.1368–1375 (2019)
(8) K. Sakata and H. Fujimoto: “Perfect Tracking Control of Servo Motor Based on Precise Model with PWM Hold and Current Loop”, Power Conversion Conference, pp.1077–1082 (2007)
(9) K. Nakamura, H. Fujimoto, and M. Fujitsuna: “Torque ripple suppression control for PM motor with high bandwidth torque meter”, 2009 IEEE Energy Conversion Congress and Exposition, pp.2572–2577 (2009)
(10) K. Nakamura, H. Fujimoto, and M. Fujitsuna: “Torque ripple suppression control for PM motor with current control based on PTC”, The 2010 International Power Electronics Conference, pp.1077–1082 (2010)
(11) T. Hara, T. Ajima, Y. Tanabe, M. Watanabe, K. Hoshino, and K. Oyama: “Analysis of Vibration and Noise in Permanent Magnet Synchronous Motors with Distributed Winding for the PWM Method”, IEEE Transactions on Industry Applications, Vol.54, No.6, pp.6042–6049 (2018)
(12) R. Saito, K. Tsuchida, and T. Yokoyama: “Digital Control of PWM Inverter Using Ultrahigh-Speed Network for Feedback Signals with Communication Disturbance Observer Based on Rocket I/O Protocol”, IEEJ Journal of Industry Applications, Vol.4, No.6, pp.752–757 (2015)
(13) S. Noguchi, M. Mae, and H. Fujimoto: “High-Bandwidth Current Control of PMSM Based on Quasi Multirate Feedforward Contol”, IEEJ International Workshop on Sensing, Actuation, Motion Control, and Optimization (2020)
(14) K.P. Gokhale, A. Kawamura, and R.G. Hoft: “Dead Beat Microprocessor Control of PWM Inverter for Sinusoidal Output Waveform Synthesis”, IEEE Transactions on Industry Applications, Vol.23, No.3, pp.901–910 (1987)
(15) M. Tomizuka: “Zero Phase Error Tracking Algorithm for Digital Control,” Journal of Dynamic Systems, Measurement, and Control, Vol.109, No.1, pp.65–68 (1987)
(16) H. Fujimoto, Y. Hori, and A. Kawamura: “Perfect tracking control based on multirate feedforward control with generalized sampling periods”, IEEE Trans. Industrial Electronics, Vol.48, No.3, pp.636–644 (2001)
(17) T. Yoshino, R. Araumi, K. Imai, and T. Yokoyama: “1 MHz multi sampling quasi multi-rate deadbeat control method with Rocket I/O network feedback”, IEEE 3rd International Future Energy Electronics Conference and ECCE Asia, pp.889–893 (2017)
(18) G.C. Goodwin, S.F. Graebe, and M.E. Salgado: “Control System Design”, Pearson Education (2001)
(19) S. Noguchi: “Study on High-Bandwidth Current Control for PMSMs from Current Reference Trajectory Oversampling and Torque Ripple Reduction”, Master Thesis, Department of Electrical Engineering and Information Systems, The University of Tokyo (2021) (in Japanese) (to be published)

Shona Noguchi (Student Member) received the B.E. degree from Waseda University in 2019. He is currently working towards the M.E. degree in the Department of Electrical Engineering and Information Systems, Graduate School of Engineering, the University of Tokyo. His research interests are in motor drive, motion control, and power electronics. He is a student member of The Institute of Electrical Engineers of Japan.

Masahiro Mae (Student Member) received the B.E. and M.S. degrees from The University of Tokyo in 2018 and 2020, respectively. He is currently working towards the Ph.D. degree in the Department of Electrical Engineering and Information Systems, Graduate School of Engineering, The University of Tokyo. His research interests are in control engineering, precision motion control, multirate control, and multi-input multi-output systems. He is a student member of the Institute of Electrical and Electronics Engineers and the Society of Instrumental and Control Engineers.

Hiroshi Fujimoto (Senior Member) received the Ph.D. degree in the Department of Electrical Engineering from the University of Tokyo in 2001. In 2001, he joined the Department of Electrical Engineering, Nagaoka University of Technology, Niigata, Japan, as a research associate. From 2002 to 2003, he was a visiting scholar in the School of Mechanical Engineering, Purdue University, U.S.A. In 2004, he joined the Department of Electrical and Computer Engineering, Yokohama National University, Yokohama, Japan, as a lecturer and he became an associate professor in 2005. He had been an associate professor of the University of Tokyo from 2010 to 2020 and became a professor from year 2021. He received the Best Paper Awards from the IEEE Transactions on Industrial Electronics in 2001 and 2013, Isao Takahashi Power Electronics Award in 2010, Best Author Prize of SICE in 2010, the Nagamori Grand Award in 2016, and First Prize Paper Award IEEE Transactions on Power Electonics in 2016. His interests are in control engineering, motion control, nano-scale servo systems, electric vehicle control, motor drive, visual servoing, and wireless motors. He is a senior member of IEE of Japan and IEEE. He is also a member of the Society of Instrument and Control Engineers, the Robotics Society of Japan, and the Society of Automotive Engineers of Japan. He is an associate editor of IEEE/ASME Transactions on Mechatronics from 2010 to 2014, IEEE Industrial Electronics Magazine from 2006, IEE of Japan Transactions on Industrial Application from 2013, and Transactions on SICE from 2013 to 2016. He is a chairperson of JSAE vehicle electrification committee from 2014 and a past chairperson of IEEE/IES Technical Committee on Motion Control from 2012 to 2013.